Molecular Therapy
Original Article

Differential Induction of Immunogenic Cell Death and Interferon Expression in Cancer Cells by Structured ssRNAs

Jaewoo Lee,[1,2] Youngju Lee,[1,2] Li Xu,[1] Rebekah White,[1,2] and Bruce A. Sullenger[1,2]

[1]Department of Surgery, Duke University, Durham, NC 27710, USA; [2]Duke Translational Research Institute, Duke University, Durham, NC 27710, USA

Activation of the RNA-sensing pattern recognition receptor (PRR) in cancer cells leads to cell death and cytokine expression. This cancer cell death releases tumor antigens and damage-associated molecular patterns (DAMPs) that induce anti-tumor immunity. However, these cytokines and DAMPs also cause adverse inflammatory and thrombotic complications that can limit the overall therapeutic benefits of PRR-targeting anti-cancer therapies. To overcome this problem, we generated and evaluated two novel and distinct ssRNA molecules (immunogenic cell-killing RNA [ICR]2 and ICR4). ICR2 and ICR4 differentially stimulated cell death and PRR signaling pathways and induced different patterns of cytokine expression in cancer and innate immune cells. Interestingly, DAMPs released from ICR2- and ICR4-treated cancer cells had distinct patterns of stimulation of innate immune receptors and coagulation. Finally, ICR2 and ICR4 inhibited in vivo tumor growth as effectively as poly(I:C). ICR2 and ICR4 are potential therapeutic agents that differentially induce cell death, immune stimulation, and coagulation when introduced into tumors.

INTRODUCTION

Pattern recognition receptors (PRRs) are immunological sensors that initiate the host defense response against infections. They are located at the cell surface, within endosomal compartments and in the cytoplasm, where they are poised to recognize different molecular signatures associated with invading pathogens.[1] Viral or bacterial RNAs are known to be potent ligands of multiple PRRs.[1] Retinoic acid-inducible gene I (RIG-I), melanoma differentiation associated gene 5 (MDA-5), RNA-activated protein kinase R (PKR), laboratory of genetics and physiology 2 (LGP2), Nacht leucine-rich repeat protein 3 (NALP3), and interferon-induced protein with tetratricopeptide repeats 1 (IFIT1) are located within the cytoplasm, where they sense specific molecular patterns within RNAs; e.g., 5′ triphosphate (5′ppp), 5′diphosphate (5′pp), and double-stranded RNA (dsRNA).[2,3] Toll-like receptors (TLRs) 3, 7, and 8 are localized to endosomal compartments and are activated by dsRNA (TLR3) and single-stranded RNA (ssRNA) (TLR7 and TLR8).[3]

In addition to anti-infectious immunity, the activation of RNA-sensing PRRs can mediate programmed cell death of infected cells, which allows the host to efficiently block viral replication by sacrificing infected cells.[4] PRR activation induces cell death not only in infected cells but also in non-infected, malignant cells. Transfection with synthetic viral dsRNA analogs, polyinosinic-polycytidylic acid (poly(I:C)), and short RNA duplex containing 5′ppp induces interferon (IFN) β production and programmed cell death of various human cancer cells, including melanoma,[5] hepatocellular carcinoma,[6] glioblastoma,[7] prostate cancer,[8] ovarian cancer,[9] breast cancer,[10] and pancreatic cancer[11] through the activation of RNA-sensing PRRs. Interestingly, RNA-induced PRR activation upregulated pro-apoptotic molecules (e.g., Noxa, Puma, and TRAIL) in tumor cells but not in non-malignant cells, which may relate to the induction of tumor-selective cell death by PRR-activating RNAs.[5,12]

Furthermore, PRR-mediated cell death engenders the release of damage-associated molecular patterns (DAMPs) (e.g., high-mobility group box 1 protein [HMGB1]), surface translocation of calreticulin, antigen uptake, and maturation of dendritic cells (DCs), suggesting that RNA-induced tumor cell death is pro-immunogenic and can result in anti-tumor immunity.[11,13,14] Type I IFNs (e.g., IFN-α and IFN-β), have a wide range of immune-stimulatory activities, including the augmentation of T helper type 1 cell responses, upregulation of major histocompatibility (MHC) class I molecules, generation of natural killer (NK) cell- and T cell-mediated cytotoxicity, and anti-tumor activities, including anti-proliferative, anti-angiogenic, and pro-apoptotic effects.[15] Thus, PRR-mediated cell death and release of type I IFN can cooperatively and synergistically induce both therapeutic and prophylactic cellular immune responses against tumors.

Currently, RNA-sensing PRR agonists have demonstrated little or no overall benefit to patients with cancers.[16,17] This failure is in part due to toxicity driven by non-specific induction of immune reactions.[18] All PRR signaling culminates in the activation of mitogen-activated

Received 25 October 2016; accepted 7 March 2017;
http://dx.doi.org/10.1016/j.ymthe.2017.03.014.

Correspondence: Bruce A. Sullenger, Department of Surgery, Duke University, MSRB2 1079, 106 Research Drive, Durham, NC 27710, USA.
E-mail: bruce.sullenegr@duke.edu
Correspondence: Jaewoo Lee, Department of Surgery, Duke University, MSRB2 1083, 106 Research Drive, Durham, NC 27710, USA.
E-mail: jaewoo.lee@duke.edu

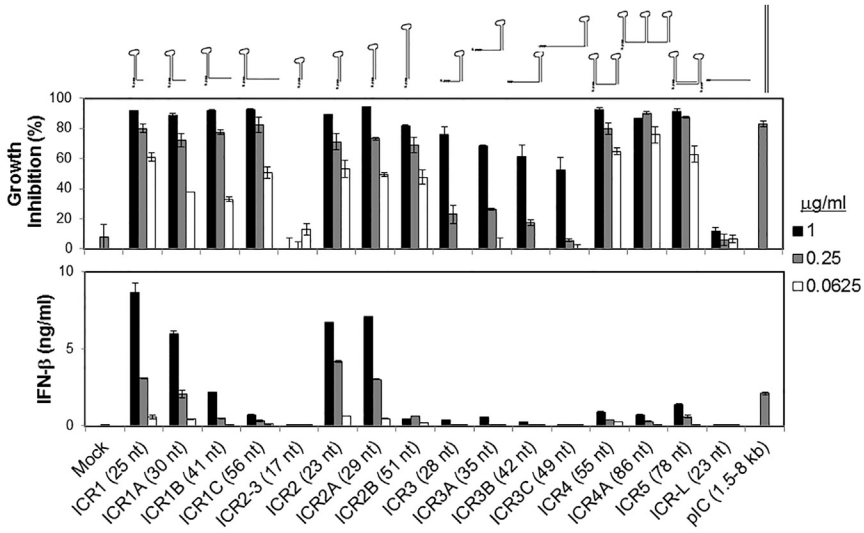

Figure 1. Differential Induction of Growth Inhibition and IFN-β Expression by 2′F-Modified 5′ppp RNAs in a Structure-Dependent Manner

2′F pyrimidine-incorporated 5′ppp RNAs were designed and generated to contain 5′ppp and various secondary structures, including a 3′ overhang hairpin (ICR1, ICR1A, ICR1B, and ICR1C), a blunt-ended hairpin (ICR2–3, ICR2, ICR2A, and ICR2B), a 5′ overhang hairpin (ICR3, ICR3A, ICR3B, and ICR3C), and multiple stem-loops (ICR4, ICR4A, and ICR5) at various lengths. Linear 5′ppp ssRNA (ICR-L) and long dsRNA (pIC) were also generated. The RNA secondary structure was predicted using mFold (http://mfold.rna.albany.edu/?q=mfold/RNA-Folding-Form). To treat cancer cells with these RNAs, WM266-4 human melanoma cells (1×10^4 cells/well) were transfected for 4 hr with the indicated concentrations of RNAs in a 96-well plate. 72 hr after RNA treatment, cells and culture supernatants were harvested and analyzed for growth inhibition and IFN-β expression, respectively. The data represent two individual experiments. Error bars show SD.

protein kinases (MAPKs), nuclear factor κB (NF-κB), and IFN regulatory factors (IRFs), which ultimately leads to the production of inflammatory cytokines and IFNs.[3] These cytokines and IFNs facilitate the induction of anti-tumor immune responses as well as cancer cell death; on the other hand, they can cause damage to normal tissues and organ failure.[15] Furthermore, the pro-inflammatory cytokines produced by tumor and tumor stroma cells promote tumor growth and survival and contribute to the deregulation of anti-tumor immunity,[19] which negatively impacts the therapeutic effects of anti-cancer PRR agonists. Therefore, the development of safe and effective RNA-sensing PRR agonists is necessary for these to become useful agents clinically.

Multiple RNA-sensing PRRs, including RIG-I,[5] MDA5,[20] TLR3,[10] and TLR7,[21] have been shown to induce programmed cell death along with cytokine expression. It is still not clear how the activation of such RNA-sensing PRRs leads to cell death in cancer cells and whether PRR-mediated cell death and cytokine expression can be uncoupled. Recently, Yu et al.[22] demonstrated that an MDA5 mutant lacking N-terminal caspase recruitment domains (CARDs) engaged a programmed cell death program in prostate cancer cells but did not induce the expression of IFN-β. However, no RNA agonists have been developed to differentially induce cell death and IFN and pro-inflammatory cytokine expression in cancer cells. In this study, we generate and screen multiple nuclease-resistant RNA molecules that can differentially induce immunogenic cancer cell death with or without concomitant expression of IFN-β and pro-inflammatory cytokines.

RESULTS

Screening of RNA Molecules for Differential Induction of Cancer Cell Death and Expression of IFN-β and Pro-inflammatory Cytokines

5′(p)pp and a short RNA duplex composed of interstranded or intrastranded base pairs (10–20 bp) are well known motifs recognized by RIG-I.[23,24] MDA5 and TLR3 are activated by long dsRNA (0.5–6 kb)[25] and short dsRNAs (>21 bp),[26] respectively, in a sequence-independent manner, whereas TLR7 is activated by AU- and GU-rich short ssRNAs in a sequence-dependent manner.[27] However, other motifs recognized by RIG-I, MDA5, TLR3, and TLR7 likely exist. We recently found that transfection with RNA aptamers containing 5′ppp and stem-loop(s) induced cell death and IFN-β expression in human melanoma cells in a RIG-I- and IPS-I-dependent manner.[28] Using the structure and sequence information of these RNA ligands, we first designed ssRNAs containing 5′ppp, AU and GU motifs, and various length and numbers of stem-loops to determine optimal RNA structures for enhancement of PRR-mediated immunogenic cell death and type I IFN expression in human cancer cells (Figure 1; Table S1). To increase the stability and cellular half-life of RNA ligands, we incorporated 2′-fluoro (2′F) pyrimidines into the RNAs. These RNAs are referred to as immunogenic cancer cell-killing RNAs (ICRs).

Transfection with ICRs containing at least one stem structure longer than 9 bp induced cytotoxicity in human melanoma cells in a dose-dependent manner, whereas linear ICRs and ICRs containing a stem structure shorter than 9 bp had no cytotoxicity in these cells (Figure 1; Figure S1). Interestingly, the 5′ overhang length but not the 3′ overhang length is inversely correlated with cytotoxicity. Unlike cytotoxicity, ICRs with a blunt end on a 9- to 12-bp-long stem-loop induced 2- to 3-fold higher production of IFN-β by human melanoma cells than poly(I:C), whereas the length of 5′ and 3′ overhangs and the number and length of stem-loops were inversely correlated with IFN-β expression in human melanoma cells (Figures 1 and 2A). To elucidate the difference between cytotoxicity and IFN-β expression patterns of different ICRs, we further investigated two representative ICRs, ICR2 and ICR4. ICR2 is a blunt-ended hairpin RNA 23 nt in length and induced high cytotoxicity and high IFN-β expression, whereas ICR4 is predicted to form a double stem-loop

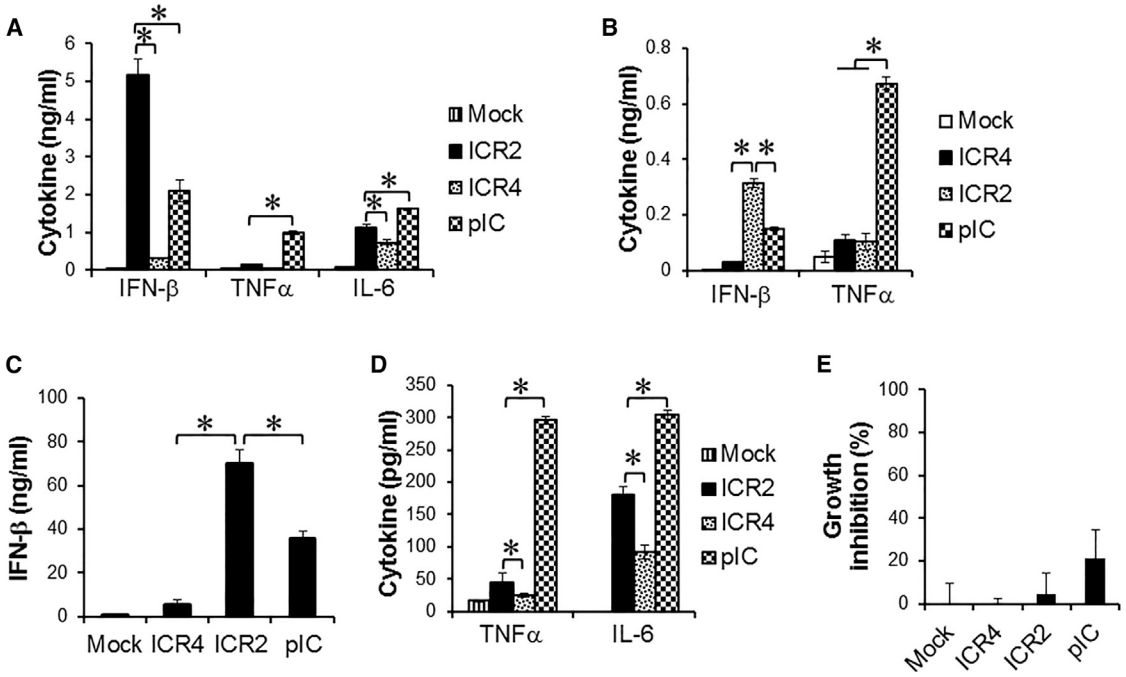

Figure 2. ICR4 Induces Decreased IFN-β and Pro-inflammatory Cytokine Expression in Human Cancer Cells and Innate Immune Cells Compared with ICR2
(A–E) WM266-4 cells (A, 1×10^4 cells/well), human PBMCs (B and E, 1×10^5 cells/well), and human DCs (C and D, 5×10^4 cells/well) were transfected for 4 hr with ICR2, ICR4, or poly(I:C) (1 μg/mL each) or transfection agent alone (Mock) in a 96-well plate. (A–D) Culture supernatants were harvested at 24 hr after transfection. (E) growth of human PBMCs was measured 3 days after transfection using an MTS assay. Data are the mean of three experiments. Error bars show SD. *$p < 0.05$.

structure 55 nt in length and induced high cytotoxicity and low IFN-β expression (Figure 1; Figure S1).

ICR2 and ICR4 Differentially Induced Expression of Pro-inflammatory Cytokines and IFN-β in Human and Mouse Cancer Cells and Innate Immune Cells

We next asked whether ICR2 and ICR4 differentially induced cytotoxicity and IFN-β expression in different types of cancer cells other than melanoma cells. Both ICR2 and ICR4 induced an over 70% decrease in proliferation of human prostate cancer cells (DU-145) and human pancreatic cancer cells (PANC-1 and BxPC3). ICR2 induced more than a 2-fold higher increase in IFN-β expression in these cells than ICR4 (Figure S2). Differential induction of IFN-β expression by ICR2 and ICR4 was also observed in innate immune cells, including human peripheral blood mononuclear cells (PBMCs) and DCs (Figures 2B and 2C). In addition to IFN-β, the expression of pro-inflammatory cytokines, e.g., tumor necrosis factor alpha (TNF-α) and interleukin-6 (IL-6, in human DCs were significantly less induced by ICR4 than ICR2 (Figure 2D). Interestingly, transfection with ICR2 induced significantly higher IFN-β expression in human cancer cells and DCs than transfection with poly(I:C), but transfection with ICR2 induced a significantly lower expression of TNF-α and IL-6 than transfection with poly(I:C) (Figures 2A–2D). In contrast to cancer cells, ICR2 and ICR4 did not induce cytotoxicity in human PBMCs (Figure 2E). Surprisingly, ICR2 did not induce cytotoxicity or expression of IFN-β, TNF-α, and IL-6 in mouse cancer cells. ICR4 induced cytotoxicity and IFN-β expression in mouse melanoma and mouse pancreatic cancer cells, although the cytotoxic effects were much less in mouse cancer cells compared with human counterparts (48.11% ± 5.365% [B16] versus 92.7075% ± 1.223% [WM266-4]; 41.59% ± 7.809% [PANC-02] versus 88.39% ± 4.470% [PANC-1]) (Figures S2 and S3).

ICR2 Induced Delayed IFN-Dependent Cell Death, whereas ICR4 Induced Acute IFN-Independent Cell Death

We next elucidated the mechanism of cytotoxicity induced by ICR2 and ICR4 in human cancer cells. Annexin V single-positive cells represent early apoptosis, whereas Annexin V and 7-aminoactinomycin D (7-AAD) double-positive cells are primary and secondary necrotic cells.[29] Early apoptosis appeared at 4 hr after transfection with ICR4 or poly(I:C), and both early apoptosis and primary and secondary necrosis gradually increased in these cells during culture (Figures 3A and 3B). In cells transfected with ICR2, no significant cell death appeared at 4 hr, and only marginal early apoptosis and necrosis appeared at 24 hr. Interestingly, cells transfected with ICR2 showed many more necrotic events than early apoptotic events at 48 hr (Figure 3A). It has been shown that T7 RNA polymerase has a RNA-dependent RNA polymerase activity, and T7 RNA polymerase-induced in vitro transcription (IVT) potentially forms non-templated self-complementary products.[23] We observed that ICR2 produced by T7 RNA polymerase-induced IVT contained both the expected length of ICR2 RNA and a longer ICR2 IVT product than

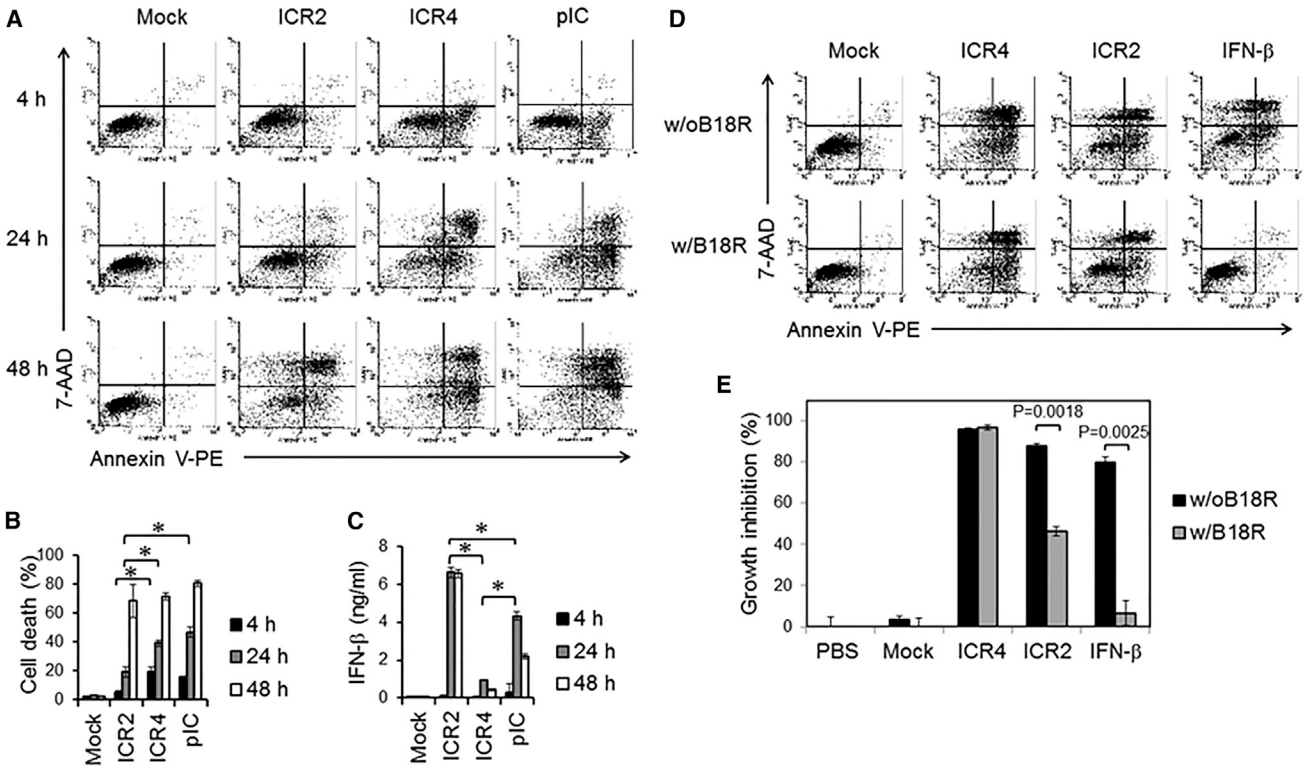

Figure 3. ICR4 and Poly(I:C) Induced Acute Cell Death, whereas ICR2 Induced Delayed Cell Death

(A–C) WM266-4 cells (2×10^5 cells/well) were transfected for 4 hr with ICR2, ICR4, or poly(I:C) (1 μg/mL each) or transfection agent alone (Mock) in a 24-well plate. Cells and culture supernatants were harvested 4, 24, and 48 hr after transfection. (A and B) Cell death was determined using Annexin V and 7-AAD staining. % Cell death = (% Annexin $V^+/7\text{-}AAD^-$) + (% Annexin $V^-/7\text{-}AAD^+$) + (% Annexin $V^+/7\text{-}AAD^+$). (C) IFN-β production was determined by ELISA. (D and E) ICR2 but not ICR4 induced IFN-dependent cell death. WM266-4 cells (1×10^4 cells/well) were transfected for 4 hr with ICR2, ICR4 (0.2 μg/mL each), or transfection agent alone (Mock) in a 96-well plate. Recombinant human IFN-β (100 ng/mL) was used as a positive control. Immediately after transfection, cells were cultured for 3 days in the presence or absence of B18R (1 μg/mL). Cytotoxicity was determined by Annexin V/7-AAD assay (D) and MTS assay (E). In (A), the data represent three individual experiments. In (D), the data represent two individual experiments. In (B), (C), and (E), the data are the mean of three experiments. Error bars show SD. *$p < 0.05$.

expected (Figure S4A). Transfection with the longer ICR2 IVT product induced pronounced cell death 24 hr after transfection (Figure S4B). To avoid non-specific cell death induced by IVT byproducts, expected-length ICRs were purified by PAGE. Unlike cell death, IFN-β production by human melanoma cells was not observed 4 hr after transfection with ICR2, ICR4, or poly(I:C). IFN-β was continuously detected 24 hr and 48 hr after transfection. Cells transfected with ICR2 produced 8- to 10-fold higher amounts of IFN-β than cells transfected with ICR4 (Figure 3C). IFN-β is known to induce cell death via multiple mechanisms, including caspase-dependent apoptosis[30] and programmed necrosis, called necroptosis.[31] Thus, we speculated that ICR2 induced IFN-dependent cancer cell death, whereas ICR4 induced IFN-independent cancer cell death. To further elucidate the mechanism(s) of IFN-dependent or -independent cell death by ICR2 and ICR4, human melanoma cells were transfected with either ICR2 or ICR4, followed by treatment with the vaccinia virus-encoded IFN α and β decoy receptor B18R. B18R significantly inhibited ICR2- and IFN-β-induced cell death but not ICR4-induced cell death (Figures 3D and 3E). These data suggest that ICR2 induces cell death, at least in part, in an IFN-dependent manner, whereas ICR4 induces apoptosis in an IFN-independent manner.

ICR2 and ICR4 Triggered Different Cell Death Mechanisms in Human Cancer Cells

We next investigated cell death mechanisms and signaling pathways in human cancer cells treated with ICR2 and ICR4. Carbobenzoxy-valyl-alanyl-aspartyl-[O- methyl]- fluoromethylketone (Z-VAD)-fmk is a pan-caspase inhibitor and is thus considered an apoptosis inhibitor. Necrostatin-1 (Nec-1) is an inhibitor of receptor-interacting serine/threonine protein kinase 1 (RIP1) and commonly used as a necroptosis inhibitor. Cell death induced by ICR4 is more inhibited by Z-VAD-fmk than by Nec-1, whereas the converse is true for ICR2 as cell death is more inhibited by Nec-1 than by Z-VAD-fmk (Figure 4A). Co-treatment with both Z-VAD-fmk and Nec-1 inhibited cancer cell death to a greater extent than single treatment with either Z-VAD-fmk or Nec-1 (Figure 4A). These data indicate that ICR2-induced cell death is much more dependent on RIP1 than caspases, whereas ICR4-induced cell death is more dependent on caspases

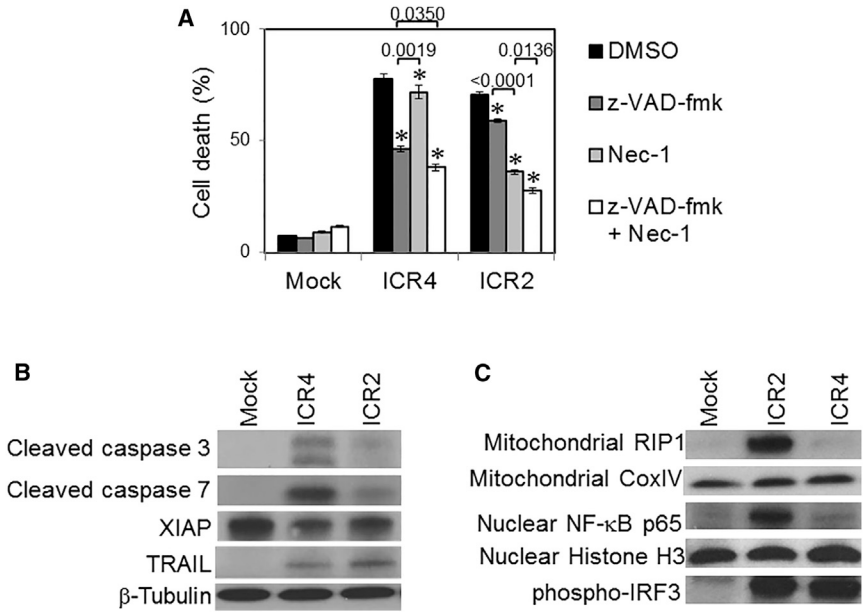

Figure 4. ICR2 and ICR4 Trigger Differential Activation of Cell Death and PRR Signaling Pathways

(A) WM266-4 cells (2×10^5 cells/well) were pre-incubated for 6 hr with Z-VAD-fmk, Nec-1, a mixture of Z-VAD-fmk and Nec-1, or DMSO, followed by transfection for 4 hr with ICR2, ICR4 (0.2 μg/mL each), or transfection agent alone (Mock). Cells were cultured for 3 days in the presence of DMSO, Z-VAD-fmk, and/or Nec-1. Cell death was determined 72 hr after transfection by Annexin V/7-AAD assay. (B and C) WM266-4 cells were harvested at 24 hr after transfection with ICR2 or ICR4 or mock transfection. Total cell lysates, mitochondrial lysates, and nuclear extracts were prepared and analyzed by western blot. (B) Expression of cell death-associated molecules, including cleaved caspase-3 and -7, XIAP, and TRAIL, in total cell lysates was assessed. β-Tubulin expression was used as a loading control. (C) The expression of mitochondrial RIP1 and cytochrome *c* oxidase IV (COX IV) in mitochondrial lysates, NF-κB, p65, and histone H3 in nuclear extracts, and phospho-IRF3 in total cell lysates was determined. Error bars represent the SD. In (A), the data are the mean of three experiments. Error bars show SD. In (B) and (C), the data represent two individual experiments. *$p < 0.05$ (versus DMSO).

than RIP1. Consistent with this result, the expression levels of cleaved caspase-3 and -7 in melanoma cells treated with ICR4 were found to be much higher than in cells treated with ICR2 (Figure 4B). In contrast, cells treated with ICR2 had significantly more RIP1 translocated in mitochondria than cells treated with ICR4 (Figure 4C). Interestingly, both ICR2 and ICR4 significantly downregulated anti-apoptotic protein X-linked inhibitor of apoptosis (XIAP) and upregulated pro-apoptotic protein TNF-related apoptosis-inducing ligand (TRAIL) in human melanoma cells (Figure 4B). These observations suggest that both ICR2 and ICR4 sensitize human cancer cells to programmed cell death by downregulation of XIAP and upregulation of TRAIL.

Differential Activation of NF-κB in Cancer Cells Treated with ICR2 and ICR4

Cells treated with ICR2 produced much more IFN-β and pro-inflammatory cytokines than cells treated with ICR4 (Figure 2). We speculated that ICR2 and ICR4 differentially activated NF-κB and IRF signaling pathways, which led to the expression of inflammatory cytokines and IFNs, respectively. NF-κB was highly detected in the nuclear fraction of cells transfected with ICR2 but only marginally detected in the nuclear fraction of cells transfected with ICR4, whereas phosphorylated IRF3 was similarly detected in cells transfected with either ICR2 or ICR4 (Figure 4C). Activation of IRF3 is known to have dual roles in anti-viral responses, including induction of apoptosis and expression of type I IFN genes.[32] Although IRF3 was equally activated by ICR2 and ICR4 in human melanoma cells, IRF3 might play different roles in cells transfected with ICR2 and ICR4. Further studies are needed to elucidate the functional activity of IRF3 in cells transfected with ICR2 and ICR4.

Activation of RNA-Sensing PRRs by ICR2 and ICR4

Our recent studies demonstrated that 2′F-modified RNA aptamers containing 5′ppp and stem-loop(s) induced programmed cell death and IFN-β production by human melanoma and hepatocellular carcinoma cells in a RIG-I-dependent manner.[28] To answer whether ICR2 and ICR4 induced RIG-I-dependent cell death of human cancer cells, we treated Huh7.0, a RIG-I-wild-type human hepatocellular carcinoma cell line, and Huh7.5, a RIG-I mutant Huh7.0 cell line, with either ICR2 or ICR4. ICR4 was cytotoxic to Huh7.0 cells but not to Huh7.5 cells (Figure 5A). Interestingly, ICR2 induced similar cytotoxicity in Huh7.0 and Huh7.5 cells. Moreover, ICR4, but not ICR2, had significantly reduced cytotoxicity in human melanoma cells with small interfering RNA (siRNA)-mediated RIG-I knockout, whereas ICR4 and ICR2 led to similar levels of cytotoxicity in human melanoma cells with knockout of other cytoplasmic RNA-sensing PRRs, including PKR and MDA5 (Figures 5B and 5C). Furthermore, human TLR3 and TLR7 reporter cells were not stimulated by ICR2 and ICR4 (Figure 5D). Removing 5′ppp of ICR2 and ICR4 by bacterial alkaline phosphatase (BAP)-induced dephosphorylation significantly prevented cell death and IFN-β production by human melanoma cells (Figures 5E and 5F). Interestingly, 2' hydroxyl (2′OH) pyrimidine-incorporated ICR4 significantly decreased cytotoxicity, but not IFN-β-inducing activity, compared with 2′F pyrimidine-incorporated ICR4, whereas 2′OH pyrimidine-incorporated ICR2 completely abrogated both cytotoxicity and IFN-β-inducing activity (Figure S5). Thus, ICR4 induced anti-cancer responses in a RIG-I-dependent but PKR- and MDA5-independent manner. By contrast, ICR2-induced anti-cancer responses did not appear to be affected by the loss of RIG-I, MDA5, or PKR.

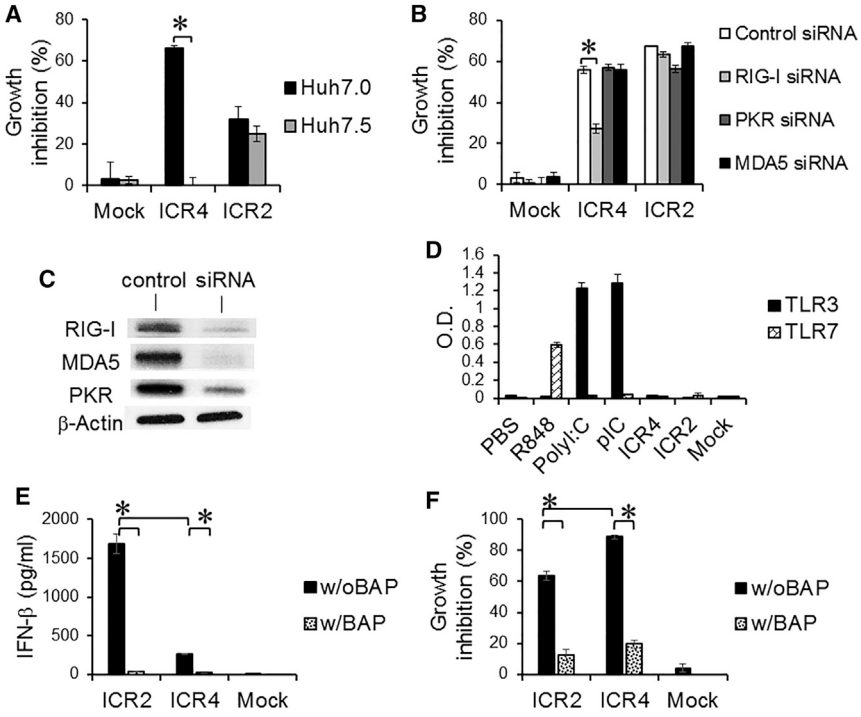

Figure 5. Induction of RNA-Sensing PRR-Mediated Cytotoxicity by ICR2 and ICR4

(A) Huh7.0 (RIG-I wild-type) and Huh7.5 (RIG-I mutant) cells (7×10^3 cells/well) were transfected with ICR2 or ICR4 (1 μg/mL each) or mock-transfected in a 96-well plate. Cytotoxicity was determined 3 days after transfection by MTS assay. (B) RIG-I, PKR, and MDA5 in WM266-4 cells were knocked down three times with siRNAs. Cells (1×10^4 cells/well) were re-plated in a 96-well plate and transfected with ICR2 or ICR4 (0.2 μg/mL each) or mock-transfected. Cytotoxicity was determined 3 days after transfection by MTS assay. (C) Knockdown of RIG-I, MDA5, and PKR in human melanoma cells. siRNA-mediated knockdown efficiency was assessed 4 days after mock transfections (control) or siRNA (lacking 5′ppp) transfections by western blot using siRNA-corresponding antibodies as indicated. β-Actin antibody was used as a loading control. (D) HEK-TLR3 and HEK-TLR7 reporter cells (4×10^4 cells/well each) were transfected with ICR2, ICR4 or poly(I:C) (pIC) (0.5 μg/mL each). Non-transfected poly(I:C) and R848 were used as positive controls for TLR3 and TLR7, respectively. PBS treatment was used as a negative control. (E and F) ICR2 and ICR4 were dephosphorylated by treatment with a BAP. The dephosphorylation was repeated twice. WM266-4 cells were transfected with BAP-treated and BAP-untreated ICR2 or ICR4 (30 nM each) or mock transfection. Cytotoxicity and IFN-β production was determined 2 days after transfection. Error bar represent SD. *$p < 0.05$.

ICR2 and ICR4 Induced Translocation of Calreticulin and HMGB1

Certain types of anti-cancer agents (e.g., doxorubicin [Dox]) can induce immunogenic cell death, characterized by the release of DAMPs, the surface expression of an "eat me" signal (e.g., the endoplasmic reticulum-residential protein Calreticulin), and the activation of innate immune cells such as DCs and NK cells.[33] This immunogenic cell death significantly contributes to the overall therapeutic outcomes of cancer therapies by the induction of anti-tumor immune responses. Both ICR2 and ICR4 slightly induced surface translocation of Calreticulin (Figure 6A). It has been shown that surface Calreticulin facilitates phagocytosis of Dox-treated cancer cells by DCs.[34] To study phagocytosis of ICR2- and ICR4-treated cancer cells by DCs, human immature DCs were incubated with human melanoma cells killed by ICR2 and ICR4, as shown in Figure 6B. These dead/dying cancer cells were taken up by DCs as effectively as cells killed by Dox. Translocation of HMGB1 from the nucleus to the cytoplasm was also observed in human melanoma cells treated with ICR2 and ICR4 (Figure S6). Interestingly, treatment with ICR2 induced significantly higher levels of HMGB1 release from human melanoma cells than treatment with ICR4 or Dox and similarly high levels as treatment with poly(I:C) (Figure 6C). Consistent with increased HMGB1 release, DAMPs generated by ICR2-indcued melanoma cell death induced significantly more activation of HMGB1-recognizing TLR4 than DAMPs generated by ICR4-induced cell death (Figure 6D) even though DAMPs released by ICR4-induced cell death were significantly more potent in stimulating TLR4 than DAMPs released by Dox-induced cell death.

ICR2 and ICR4 Induced the Release of Innate Immune-Stimulatory and Pro-coagulant DAMPs from Human Cancer Cells

To elucidate whether DAMPs released from cancer cells treated with ICR2 and ICR4 stimulate other TLRs, we collected and incubated DAMPs released from dead/dying human melanoma cells with TLR2, TLR3, and TLR9 reporter cells. The levels of activation of these TLR reporter cells were not significantly different between DAMPs released from ICR2-treated cells and from poly(I:C)-treated cells. DAMPs released from ICR2-treated cells, however, more potently activated TLR reporter cells than DAMPs released from ICR4-treated cells. ICR4-treated cells induced significantly higher TLR3 activation than Dox-treated cells (Figure 6E), whereas ICR4-treated cells induced significantly less TLR2 and TLR9 activation than Dox-treated cells (Figures 6F and 6G). These DAMPs released from ICR2- and ICR4-treated cancer cells stimulated immature human DCs to produce cytokines (Figure S7). In addition to immune-stimulatory activities, DAMPs are known to facilitate hemostasis and thrombosis[35] and may play an important role in tumor recurrence and metastasis after anti-cancer therapies.[36] Interestingly, DAMPs released from ICR2- and poly(I:C)-treated human melanoma cells activated coagulation of plasma compared with DAMPs released from mock-transfected cells, whereas DAMPs released from ICR4- and Dox-treated melanoma cells did not significantly change plasma coagulation times (Figure S8). These data suggested that ICR4-treated cancer cells released lower amounts of innate immune stimulators and pro-coagulants than ICR2-treated cells.

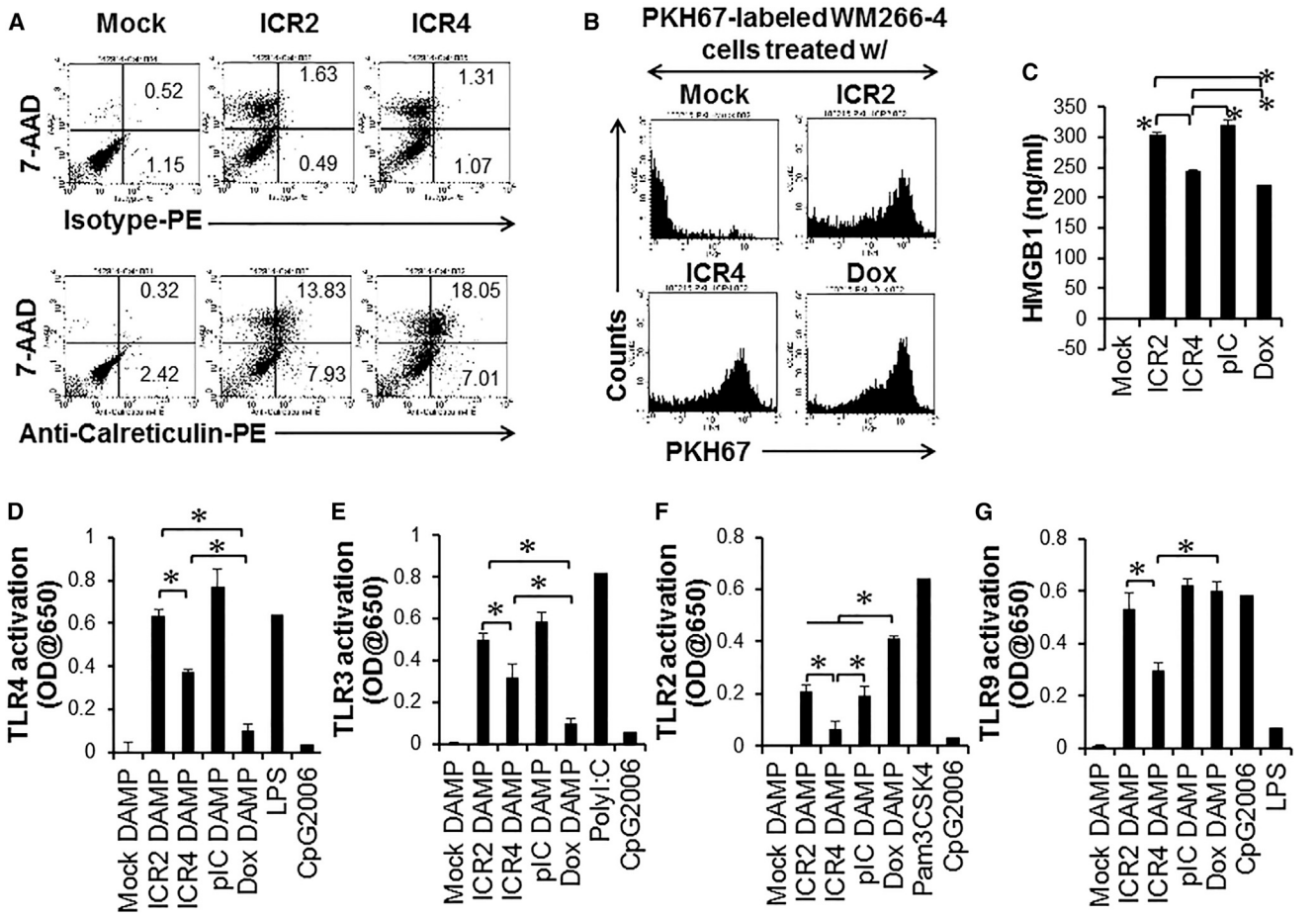

Figure 6. Release of Innate Immune-Stimulatory DAMPs and Calreticulin from Human Cancer Cells after Treatments with Immunogenic Cell Death-Inducing Agents

(A) WM266-4 cells (2×10^5 cells/well) were transfected with ICR2 or ICR4 (0.5 μg/mL each) in a 24-well plate and harvested 24 hr after transfection. Surface expression of Calreticulin was determined by flow cytometry. (B) Uptake of dead/dying WM266-4 cells treated with ICR2, ICR4, or Dox by DCs was determined by phagocytosis assay. (C) Secretion of nuclear protein HMGB1 from cells treated with ICR2, ICR4, or Dox was determined by ELISA. (D–G) DAMPs were isolated from WM266-4 cells treated with transfection agent alone (Mock DAMP), ICR2 (ICR2 DAMP), ICR4 (ICR4 DAMP), poly(I:C) (pIC DAMP), or Dox (Dox DAMP) as described in Materials and Methods. HEK-TLR2, HEK-TLR3, HEK-TLR4, and HEK-TLR9 reporter cells (5×10^4 cells/well) were incubated with DAMPs (25% v/v). Activation of TLRs was determined by colorimetric assay. Pam3CSK4, non-transfected poly(I:C), LPS, and CpG 2006 were used as positive controls in TLR reporter assays. In (A) and (B), the data represent two individual experiments. In (C)–(G), the data are the mean of three experiments. Error bars show SD. *$p < 0.05$.

In Vivo Transfection with ICR2 and ICR4 Extended Survival in Melanoma-Bearing Mice

Finally, we evaluated the in vivo therapeutic efficacy of ICR2 and ICR4 in a human melanoma xenograft model. Repeated intratumoral treatments with ICR2 or ICR4 inhibited tumor growth (Figure 7A) and significantly enhanced survival in nude mice with subcutaneous human melanoma xenografts (Figure 7B). A trend toward a reduced therapeutic effect of ICR4 compared with ICR2 and the gold-standard PRR-stimulating RNA agonist poly(I:C) was observed; however, the difference between ICR2, ICR4, and poly(I:C) was not statistically significant. In immunocompetent mice bearing B16 mouse melanoma, ICR4 treatment appeared to be significantly less therapeutically effective than poly(I:C) treatment (Figure 7C).

DISCUSSION

PRR-induced cancer cell death accompanies the release of multiple immune and hemostatic modulators (e.g., IFNs, inflammatory cytokines, and DAMPs) that orchestrate the stimulation of innate and adaptive immune responses against cancer and also, potentially, cause destructive inflammatory responses against normal tissues and thrombotic complications. It has long been asked how the dichotomous responses generated by PRR-induced cancer cell death are favorably modified to enhance the anti-cancer therapeutic effects and overall benefits of PRR therapeutics. Both ICR2 and ICR4 are novel PRR-stimulating ssRNAs that provoked strong immunogenic cell death of human cancer cells and significantly reduced TNF-α production by human cancer and immune cells compared with poly(I:C).

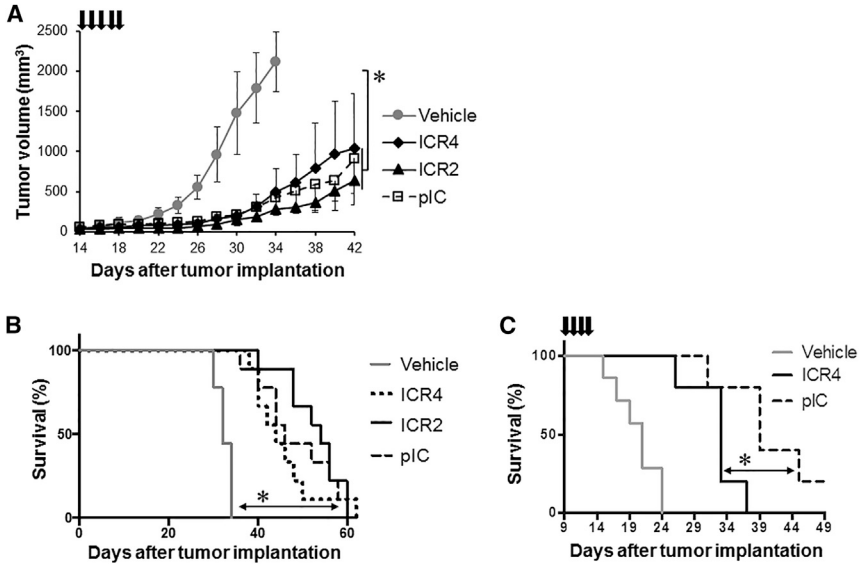

Figure 7. Inhibition of Tumor Growth by ICR2 and ICR4

(A and B) Human melanoma WM266-4 cells (7×10^5) were injected subcutaneously into a nude mouse. Tumor-bearing mice were intratumorally injected daily for 5 consecutive days with ICR2, ICR4, or pIC (20 μg/mouse each) using in vivo-jetPEI (n = 9). (C) B16-F0 mouse melanoma cells (2×10^5) were injected subcutaneously into a syngeneic C57BL/6 mouse. Either ICR4 or pIC (20 μg/mouse each) was administered intratumorally for 4 consecutive days (n = 5). Tumor growth (A) was measured every other day, and the survival rate (B and C) was determined. Error bars show SD. *$p < 0.05$ (vehicle versus ICR2, ICR4, and pIC).

ICR2 induced IFN-dependent necroptosis of human cancer cells and much higher amounts of type I IFN than ICR4. In contrast, ICR4 induced RIG-I-dependent apoptotic cell death and generated significantly fewer inflammatory and less coagulative DAMPs than ICR2.

It has been thought that physiological cell death such as apoptosis is poorly immunogenic or tolerogenic, whereas pathological death such as necrosis is immunogenic.[37] However, it has also been shown that certain apoptotic agents (e.g., Dox), induced more immunogenic cancer cell death than necrotic agents.[34,38] It is still unclear how the immune system differentially responds to different types of cancer cell death. Although the types of TLRs stimulated by ICR4-generated DAMPs were similar to those stimulated by ICR2- and poly(I:C)-generated DAMPs, the signal strength of TLRs stimulated by ICR4-generated DAMPs was significantly lower than that of TLRs stimulated by ICR2- and poly(I:C)-generated DAMPs. Consistent with TLR signal strength, ICR4-induced cell death released significantly fewer amounts of the endogenous TLR4 ligand HMGB1 than ICR2- and poly(I:C)-induced cell death.

However, the levels of DAMPs are not always directly correlated with the immunogenicity and TLR-stimulatory activity of cell death. Both ICR4 and Dox induced apoptotic cancer cell death, and they produced comparable amounts of HMGB1 release. However, TLR4 reporter cells were stimulated by ICR4-generated DAMPs but not by Dox-generated DAMPs. Depending on the oxidative state, HMGB1 was shown to differentially induce innate and inflammatory responses.[39] Reduced HMGB1 is able to stimulate TLR4 and has immune-stimulatory activity, but oxidized HMGB1 does not stimulate TLR4 and has tolerogenic activity.[39,40] These data suggest that different types of cell death may generate quantitatively and qualitatively different DAMPs and lead to different types of TLR stimulation and different immune responses.

Kohlway et al.[24] demonstrated that a 5′ppp RNA hairpin with a duplex length of 10 bp effectively stimulated RIG-I ATPase activity in vitro, and transfection with this RNA hairpin induced IFN-β production by the RIG-I-expressing 293T cell line. ICR2 is a 2′F-modified 5′ppp RNA hairpin with a duplex length of 9 bp. The secondary structure of ICR2 is very similar to Kohlway's RNA hairpin. However, ICR2 does not contain known RIG-I stimulating motifs (e.g., U/UC),[41] whereas Kohlway's RNA has a U/UC motif. We demonstrated that treatment with ICR2 showed comparable cytotoxicity to both the Huh7.0 and RIG-I-deficient Huh7.5 cell lines. Furthermore, ICR2-induced cancer cell death and IFN-β expression were not significantly affected by the deficiency of individual RIG-I, MDA5, and PKR. One possibility is that ICR2 may be recognized by other RNA-sensing PRRs. For example, TLR13 is an endosomal TLR whose functions and ligands remain poorly understood. A recent study has demonstrated that a virus-derived 16-nt ssRNA predicted to form a stem-loop structure stimulated mouse TLR13.[42] The human TLR13 gene and its anti-cancer activities have not yet been elucidated. Nucleotide-binding oligomerization domain 2 (NOD2) is another cytoplasmic PRR that recognizes bacterial peptidoglycan as well as viral ssRNAs.[43] NOD2 triggers activation of IRF3 and expression of IFN-β in human and mouse cells.[44] Furthermore, IFIT1 selectively binds to 5′ppp RNA in a sequence-independent manner and induces anti-viral responses.[2] Another possibility is that multiple RNA-sensing PRRs may simultaneously recognize ICR2 and play compensatory roles in ICR2-induced IFN-β expression and cell death. Further studies are needed to elucidate the mechanism(s) of ICR2-induced innate immune stimulation and cancer cell death.

A recent study has demonstrated that combination of immunogenic cell death-inducing cancer therapeutics and checkpoint inhibitors (e.g., anti-CTLA4 and anti-PD-L1) synergistically enhanced anti-tumor response and anti-tumor immunity.[45] ICR2 and ICR4 are potent PRR-stimulating cytotoxic agents against human cancers. ICR2 and ICR4 have distinctive immune-stimulatory and hemostatic activities. Combination of dual checkpoint inhibitors and ICR4 and/or ICR2 would be a potent and effective therapy for advanced cancers.

MATERIALS AND METHODS

Cell Culture

The human melanoma cell line WM266-4 (ATCC) was maintained in Eagle's minimum essential medium supplemented with 10% fetal bovine serum (FBS), 1× non-essential amino acid (NEAA), and 1 mM sodium pyruvate (all from Invitrogen). The human prostate cancer cell line DU145 (ATCC) was cultured in DMEM (Invitrogen) supplemented with 1× NEAA, 1 mM sodium pyruvate, and 10% FBS. The human hepatocellular carcinoma cell lines Huh7.0 and Huh7.5 were kindly provided by Dr. Stacy M. Horner (Duke University). Huh7.0 cells, Huh7.5 cells, the human pancreatic cancer cell line PANC-1 (ATCC), the murine pancreatic cancer cell line PANC-02 (NIH), and the murine melanoma cell line B16.F0 (ATCC) were maintained in DMEM supplemented with 10% FBS. The human pancreatic cancer cell line BxPC3 was maintained in RPMI 1640 (Invitrogen) with 10% FBS and 2 mM L-glutamine. The TLR reporter cell lines HEK-Blue Null, HEK-Blue hTLR2, HEK-Blue hTLR3, HEK-Blue hTLR4, and HEK-Blue hTLR9 (all purchased from InvivoGen) stably express an NF-κB/AP-1-inducible secreted embryonic alkaline phosphatase (SEAP) and corresponding TLR, and these cells were maintained by following the manufacturer's instructions. Human normal PBMCs (STEMCELL Technologies) were cultured in RPMI 1640 with 10% FBS and 2 mM L-glutamine. Immature DCs were generated from PBMCs as described previously.[46] All cells were incubated at 37°C in a humidified atmosphere with 5% CO_2.

Generation of ICRs

All ICRs were produced by in vitro transcription from DNA templates using the Y639F mutant T7 RNA polymerase, followed by gel purification, as described previously.[28] All pyrimidines in the ICRs were 2′-fluoro-modified.

In Vitro RNA Treatment and PRR Stimulation

ICRs and poly(I:C) were transfected with DharmaFECT Duo liposomal transfection reagent (Thermo Scientific) at a transfection reagent (microliter):RNA (microgram) ratio of 3:1 according to the manufacturer's instructions. RNAs were transfected into 80%–90% confluent cells. Cells were incubated with an RNA-transfection agent complex for 4 hr, followed by replenishment with fresh culture medium. Cells and culture supernatants were harvested at various time points. Pam3CSK4, CpG 2006, poly(I:C), and R848 (all from InvivoGen) and lipopolysaccharide (LPS; Sigma) were used as control TLR and PRR agonists.

Quantification of Cell Growth Inhibition and Cell Death

Growth inhibition relative to untreated cells was quantified 72 hr after treatment using the Celltiter 96 3-(4,5-dimethylthiazol-2-yl)-5-(3-carboxymethoxyphenyl)-2-(4-sulfophenyl)-2H-tetrazolium (MTS) cell proliferation assay kit (Promega) according to the manufacturer's instructions. The percent growth inhibition was calculated by using the following equation: percent growth inhibition = $([O.D.]_{untreated} - [O.D.]_{treated})/[O.D.]_{untreated} \times 100$, where O.D. is optical density. Cell death was measured using the phycoerythrin (PE) Annexin V Apoptosis Detection Kit I (BD Biosciences).

Inhibition of Type I IFNs, RIP Kinase, and Caspases

Cells were treated with the type I IFN decoy receptor B18R (1 μg/mL, eBioscience), the receptor-interacting serine/threonine-protein (RIP) kinase inhibitor necrostatin-1 (100 μM, Sigma), and the pan-caspase inhibitor Z-VAD-fmk (50 μM, InvivoGen) for 6 hr before and immediately after RNA treatment. To induce IFN-β-dependent cell death, cells were treated with recombinant human IFN-β (100 ng/ml) (PeproTech).

siRNA Knockdown of RIG-I, PKR, and MDA5 Expression

Transient knockdown of RIG-I, PKR, and MDA5 was performed as described previously.[28] 5 hr after the second siRNA transfection, cells were harvested, replated into a 96-well plate, and incubated overnight. Cells were then treated with PRR-activating RNAs.

Generation of DAMPs

To generate DAMPs, 5×10^5 WM266-4 cells were transfected with RNAs (1 μg/mL) or incubated with Dox (7.5 μM, Sigma). After 4 hr, cells were washed five times with fresh culture medium and incubated for 2–3 days in 1 mL of culture medium. Dead cells were counted using trypan blue. When over 95% of cells were dead, culture supernatants were collected by centrifugation for 5 min at 1,200 rpm and stored at −80°C until use.

Phagocytosis Assay

Cells were labeled using the PKH67 green fluorescent cell linker kit (Sigma). PKH67-labeled cells were killed using RNAs or Dox (7.5 μM, Sigma). Dead/dying cells were harvested 48 hr after treatment and incubated for 1 hr with immature DCs. Phagocytosis of PKH67-labeled dead/dying cells was determined by flow cytometry.

DAMP-Induced TLR Activation and DC Stimulation

DAMPs were diluted to 25% (v/v) with complete medium. 5×10^4 TLR reporter cells or 1×10^5 immature DCs were incubated overnight with diluted DAMPs in a 96-well plate. To determine TLR activation, the level of SEAP release was determined using a colorimetric assay. Briefly, 40 μL of culture supernatants was harvested and incubated for 3 hr with 180 μL of QUANTI-Blue (InvivoGen) in a flat-bottom 96-well plate. SEAP activity was accessed by reading the optical density (OD) at 650 nm with a Power Wave XS2 ELISA plate reader (BioTek Instruments). Pam3CSK4 (a TLR2 agonist), CpG 2006 (a TLR9 agonist), poly(I:C) (a TLR3 agonist), and LPS (all from InvivoGen) were used as control TLR stimulators. To determine DC stimulation, cytokine production by DCs was determined by ELISA.

In Vivo Anti-tumor Therapy

5- to 6-week-old NU/J mice were obtained from The Jackson Laboratory. 7×10^5 WM266-4 human melanoma cells were implanted subcutaneously into the right flank of a NU/J nude mouse. When mice had a palpable tumor, the tumor-bearing mice were intratumorally

injected with 20 μg of RNA molecules using in vivo-jetPEI (Polyplus Transfection) at amine to phosphate ratio (N/P) = 8. RNAs were injected daily for 5 consecutive days. Tumor growth was evaluated every other day by measuring the tumor diameter using a caliper. Tumor volume was defined as [(width)2 × (length)]/2. Mice bearing a tumor volume exceeding 2,000 mm^3 were euthanized. All experimental procedures involving the use of mice were performed in accordance with the guidelines of and in compliance with the Animal Care and Use Committee of Duke University.

Statistical Analysis

The difference in cell growth, cell death, cytokine production, and tumor volume among experimental groups was compared using two-tailed Student's t test. Significance of survival was determined by log-rank (Mantel-Cox) test. $p < 0.05$ was used for statistical significance.

SUPPLEMENTAL INFORMATION

Supplemental Information includes Supplemental Materials and Methods, eight figures, and one table and can be found with this article online at http://dx.doi.org/10.1016/j.ymthe.2017.03.014.

AUTHOR CONTRIBUTIONS

J.L., Y.L., and L.X. designed and performed the experiments. J.L., R.W., and B.A.S. interpreted the data. J.L., R.W., and B.A.S. wrote the manuscript.

CONFLICTS OF INTEREST

The authors declare no conflict of interest.

ACKNOWLEDGMENTS

We thank Dr. Dani Bolognesi for editing and critical comments on this manuscript. This work was supported in part by the Duke University Department of Surgery (Clarence Gardner Award to J.L. and R.W.), a pilot grant from the Opportunity Funds Management Core of the Centers for Medical Countermeasures against Radiation, National Institute of Allergy and Infectious Diseases grant U19AI067773 (to J.L.), and NIH grant U54HL112307 (to B.A.S.).

REFERENCES

1. Pandey, S., Kawai, T., and Akira, S. (2014). Microbial sensing by Toll-like receptors and intracellular nucleic acid sensors. Cold Spring Harb. Perspect. Biol. *7*, a016246.
2. Pichlmair, A., Lassnig, C., Eberle, C.A., Górna, M.W., Baumann, C.L., Burkard, T.R., Bürckstümmer, T., Stefanovic, A., Krieger, S., Bennett, K.L., et al. (2011). IFIT1 is an antiviral protein that recognizes 5′-triphosphate RNA. Nat. Immunol. *12*, 624–630.
3. Jensen, S., and Thomsen, A.R. (2012). Sensing of RNA viruses: a review of innate immune receptors involved in recognizing RNA virus invasion. J. Virol. *86*, 2900–2910.
4. Blander, J.M. (2014). A long-awaited merger of the pathways mediating host defence and programmed cell death. Nat. Rev. Immunol. *14*, 601–618.
5. Besch, R., Poeck, H., Hohenauer, T., Senft, D., Häcker, G., Berking, C., Hornung, V., Endres, S., Ruzicka, T., Rothenfusser, S., and Hartmann, G. (2009). Proapoptotic signaling induced by RIG-I and MDA-5 results in type I interferon-independent apoptosis in human melanoma cells. J. Clin. Invest. *119*, 2399–2411.
6. Peng, S., Geng, J., Sun, R., Tian, Z., and Wei, H. (2009). Polyinosinic-polycytidylic acid liposome induces human hepatoma cells apoptosis which correlates to the up-regulation of RIG-I like receptors. Cancer Sci. *100*, 529–536.
7. Glas, M., Coch, C., Trageser, D., Dassler, J., Simon, M., Koch, P., Mertens, J., Quandel, T., Gorris, R., Reinartz, R., et al. (2013). Targeting the cytosolic innate immune receptors RIG-I and MDA5 effectively counteracts cancer cell heterogeneity in glioblastoma. Stem Cells *31*, 1064–1074.
8. Palchetti, S., Starace, D., De Cesaris, P., Filippini, A., Ziparo, E., and Riccioli, A. (2015). Transfected poly(I:C) activates different dsRNA receptors, leading to apoptosis or immunoadjuvant response in androgen-independent prostate cancer cells. J. Biol. Chem. *290*, 5470–5483.
9. Kübler, K., tho Pesch, C., Gehrke, N., Riemann, S., Dassler, J., Coch, C., Landsberg, J., Wimmenauer, V., Pölcher, M., Rudlowski, C., et al. (2011). Immunogenic cell death of human ovarian cancer cells induced by cytosolic poly(I:C) leads to myeloid cell maturation and activates NK cells. Eur. J. Immunol. *41*, 3028–3039.
10. Salaun, B., Coste, I., Rissoan, M.C., Lebecque, S.J., and Renno, T. (2006). TLR3 can directly trigger apoptosis in human cancer cells. J. Immunol. *176*, 4894–4901.
11. Duewell, P., Steger, A., Lohr, H., Bourhis, H., Hoelz, H., Kirchleitner, S.V., Stieg, M.R., Grassmann, S., Kobold, S., Siveke, J.T., et al. (2014). RIG-I-like helicases induce immunogenic cell death of pancreatic cancer cells and sensitize tumors toward killing by CD8(+) T cells. Cell Death Differ. *21*, 1825–1837.
12. Matsushima-Miyagi, T., Hatano, K., Nomura, M., Li-Wen, L., Nishikawa, T., Saga, K., Shimbo, T., and Kaneda, Y. (2012). TRAIL and Noxa are selectively upregulated in prostate cancer cells downstream of the RIG-I/MAVS signaling pathway by nonreplicating Sendai virus particles. Clin. Cancer Res. *18*, 6271–6283.
13. Kübler, K., Gehrke, N., Riemann, S., Böhnert, V., Zillinger, T., Hartmann, E., Pölcher, M., Rudlowski, C., Kuhn, W., Hartmann, G., and Barchet, W. (2010). Targeted activation of RNA helicase retinoic acid-inducible gene-I induces proimmunogenic apoptosis of human ovarian cancer cells. Cancer Res. *70*, 5293–5304.
14. Lion, E., Anguille, S., Berneman, Z.N., Smits, E.L., and Van Tendeloo, V.F. (2011). Poly(I:C) enhances the susceptibility of leukemic cells to NK cell cytotoxicity and phagocytosis by DC. PLoS ONE *6*, e20952.
15. Trinchieri, G. (2010). Type I interferon: friend or foe? J. Exp. Med. *207*, 2053–2063.
16. Lampkin, B.C., Levine, A.S., Levy, H., Krivit, W., and Hammond, D. (1985). Phase II trial of a complex polyriboinosinic-polyribocytidylic acid with poly-L-lysine and carboxymethyl cellulose in the treatment of children with acute leukemia and neuroblastoma: a report from the Children's Cancer Study Group. Cancer Res. *45*, 5904–5909.
17. Vacchelli, E., Eggermont, A., Sautès-Fridman, C., Galon, J., Zitvogel, L., Kroemer, G., and Galluzzi, L. (2013). Trial Watch: Toll-like receptor agonists for cancer therapy. OncoImmunology *2*, e25238.
18. Kaczanowska, S., Joseph, A.M., and Davila, E. (2013). TLR agonists: our best frenemy in cancer immunotherapy. J. Leukoc. Biol. *93*, 847–863.
19. Mumm, J.B., and Oft, M. (2008). Cytokine-based transformation of immune surveillance into tumor-promoting inflammation. Oncogene *27*, 5913–5919.
20. Duewell, P., Beller, E., Kirchleitner, S.V., Adunka, T., Bourhis, H., Siveke, J., Mayr, D., Kobold, S., Endres, S., and Schnurr, M. (2015). Targeted activation of melanoma differentiation-associated protein 5 (MDA5) for immunotherapy of pancreatic carcinoma. OncoImmunology *4*, e1029698.
21. He, W.A., Calore, F., Londhe, P., Canella, A., Guttridge, D.C., and Croce, C.M. (2014). Microvesicles containing miRNAs promote muscle cell death in cancer cachexia via TLR7. Proc. Natl. Acad. Sci. USA *111*, 4525–4529.
22. Yu, X., Wang, H., Li, X., Guo, C., Yuan, F., Fisher, P.B., and Wang, X.Y. (2016). Activation of the MDA5-IPS1 viral sensing pathway induces cancer cell death and type I interferon-dependent antitumor immunity. Cancer Res. *76*, 2166–2176.
23. Schmidt, A., Schwerd, T., Hamm, W., Hellmuth, J.C., Cui, S., Wenzel, M., Hoffmann, F.S., Michallet, M.C., Besch, R., Hopfner, K.P., et al. (2009). 5′-triphosphate RNA requires base-paired structures to activate antiviral signaling via RIG-I. Proc. Natl. Acad. Sci. USA *106*, 12067–12072.
24. Kohlway, A., Luo, D., Rawling, D.C., Ding, S.C., and Pyle, A.M. (2013). Defining the functional determinants for RNA surveillance by RIG-I. EMBO Rep. *14*, 772–779.
25. Kato, H., Takeuchi, O., Mikamo-Satoh, E., Hirai, R., Kawai, T., Matsushita, K., Hiiragi, A., Dermody, T.S., Fujita, T., and Akira, S. (2008). Length-dependent recognition of double-stranded ribonucleic acids by retinoic acid-inducible gene-I and melanoma differentiation-associated gene 5. J. Exp. Med. *205*, 1601–1610.

26. Kleinman, M.E., Yamada, K., Takeda, A., Chandrasekaran, V., Nozaki, M., Baffi, J.Z., Albuquerque, R.J., Yamasaki, S., Itaya, M., Pan, Y., et al. (2008). Sequence- and target-independent angiogenesis suppression by siRNA via TLR3. Nature *452*, 591–597.

27. Heil, F., Hemmi, H., Hochrein, H., Ampenberger, F., Kirschning, C., Akira, S., Lipford, G., Wagner, H., and Bauer, S. (2004). Species-specific recognition of single-stranded RNA via toll-like receptor 7 and 8. Science *303*, 1526–1529.

28. Lee, Y., Urban, J.H., Xu, L., Sullenger, B.A., and Lee, J. (2016). 2'Fluoro Modification Differentially Modulates the Ability of RNAs to Activate Pattern Recognition Receptors. Nucleic Acid Ther. *26*, 173–182.

29. Vermes, I., Haanen, C., Steffens-Nakken, H., and Reutelingsperger, C. (1995). A novel assay for apoptosis. Flow cytometric detection of phosphatidylserine expression on early apoptotic cells using fluorescein labelled Annexin V. J. Immunol. Methods *184*, 39–51.

30. Chawla-Sarkar, M., Leaman, D.W., and Borden, E.C. (2001). Preferential induction of apoptosis by interferon (IFN)-beta compared with IFN-alpha2: correlation with TRAIL/Apo2L induction in melanoma cell lines. Clin. Cancer Res. *7*, 1821–1831.

31. Robinson, N., McComb, S., Mulligan, R., Dudani, R., Krishnan, L., and Sad, S. (2012). Type I interferon induces necroptosis in macrophages during infection with Salmonella enterica serovar Typhimurium. Nat. Immunol. *13*, 954–962.

32. Chattopadhyay, S., Marques, J.T., Yamashita, M., Peters, K.L., Smith, K., Desai, A., Williams, B.R., and Sen, G.C. (2010). Viral apoptosis is induced by IRF-3-mediated activation of Bax. EMBO J. *29*, 1762–1773.

33. Kroemer, G., Galluzzi, L., Kepp, O., and Zitvogel, L. (2013). Immunogenic cell death in cancer therapy. Annu. Rev. Immunol. *31*, 51–72.

34. Obeid, M., Tesniere, A., Ghiringhelli, F., Fimia, G.M., Apetoh, L., Perfettini, J.L., Castedo, M., Mignot, G., Panaretakis, T., Casares, N., et al. (2007). Calreticulin exposure dictates the immunogenicity of cancer cell death. Nat. Med. *13*, 54–61.

35. Gando, S., and Otomo, Y. (2015). Local hemostasis, immunothrombosis, and systemic disseminated intravascular coagulation in trauma and traumatic shock. Crit. Care *19*, 72.

36. Alonso, D.F., Ripoll, G.V., Garona, J., Iannucci, N.B., and Gomez, D.E. (2011). Metastasis: recent discoveries and novel perioperative treatment strategies with particular interest in the hemostatic compound desmopressin. Curr. Pharm. Biotechnol. *12*, 1974–1980.

37. Green, D.R., Ferguson, T., Zitvogel, L., and Kroemer, G. (2009). Immunogenic and tolerogenic cell death. Nat. Rev. Immunol. *9*, 353–363.

38. Casares, N., Pequignot, M.O., Tesniere, A., Ghiringhelli, F., Roux, S., Chaput, N., Schmitt, E., Hamai, A., Hervas-Stubbs, S., Obeid, M., et al. (2005). Caspase-dependent immunogenicity of doxorubicin-induced tumor cell death. J. Exp. Med. *202*, 1691–1701.

39. Kazama, H., Ricci, J.E., Herndon, J.M., Hoppe, G., Green, D.R., and Ferguson, T.A. (2008). Induction of immunological tolerance by apoptotic cells requires caspase-dependent oxidation of high-mobility group box-1 protein. Immunity *29*, 21–32.

40. Yang, H., Antoine, D.J., Andersson, U., and Tracey, K.J. (2013). The many faces of HMGB1: molecular structure-functional activity in inflammation, apoptosis, and chemotaxis. J. Leukoc. Biol. *93*, 865–873.

41. Uzri, D., and Gehrke, L. (2009). Nucleotide sequences and modifications that determine RIG-I/RNA binding and signaling activities. J. Virol. *83*, 4174–4184.

42. Song, W., Wang, J., Han, Z., Zhang, Y., Zhang, H., Wang, W., Chang, J., Xia, B., Fan, S., Zhang, D., et al. (2015). Structural basis for specific recognition of single-stranded RNA by Toll-like receptor 13. Nat. Struct. Mol. Biol. *22*, 782–787.

43. Strober, W., and Watanabe, T. (2011). NOD2, an intracellular innate immune sensor involved in host defense and Crohn's disease. Mucosal Immunol. *4*, 484–495.

44. Sabbah, A., Chang, T.H., Harnack, R., Frohlich, V., Tominaga, K., Dube, P.H., Xiang, Y., and Bose, S. (2009). Activation of innate immune antiviral responses by Nod2. Nat. Immunol. *10*, 1073–1080.

45. Twyman-Saint Victor, C., Rech, A.J., Maity, A., Rengan, R., Pauken, K.E., Stelekati, E., Benci, J.L., Xu, B., Dada, H., Odorizzi, P.M., et al. (2015). Radiation and dual checkpoint blockade activate non-redundant immune mechanisms in cancer. Nature *520*, 373–377.

46. Lee, J., Boczkowski, D., and Nair, S. (2013). Programming human dendritic cells with mRNA. Methods Mol. Biol. *969*, 111–125.

YMTHE, Volume *25*

Supplemental Information

Differential Induction of Immunogenic Cell Death and Interferon Expression in Cancer Cells by Structured ssRNAs

Jaewoo Lee, Youngju Lee, Li Xu, Rebekah White, and Bruce A. Sullenger

Supplemental Figures and Legends

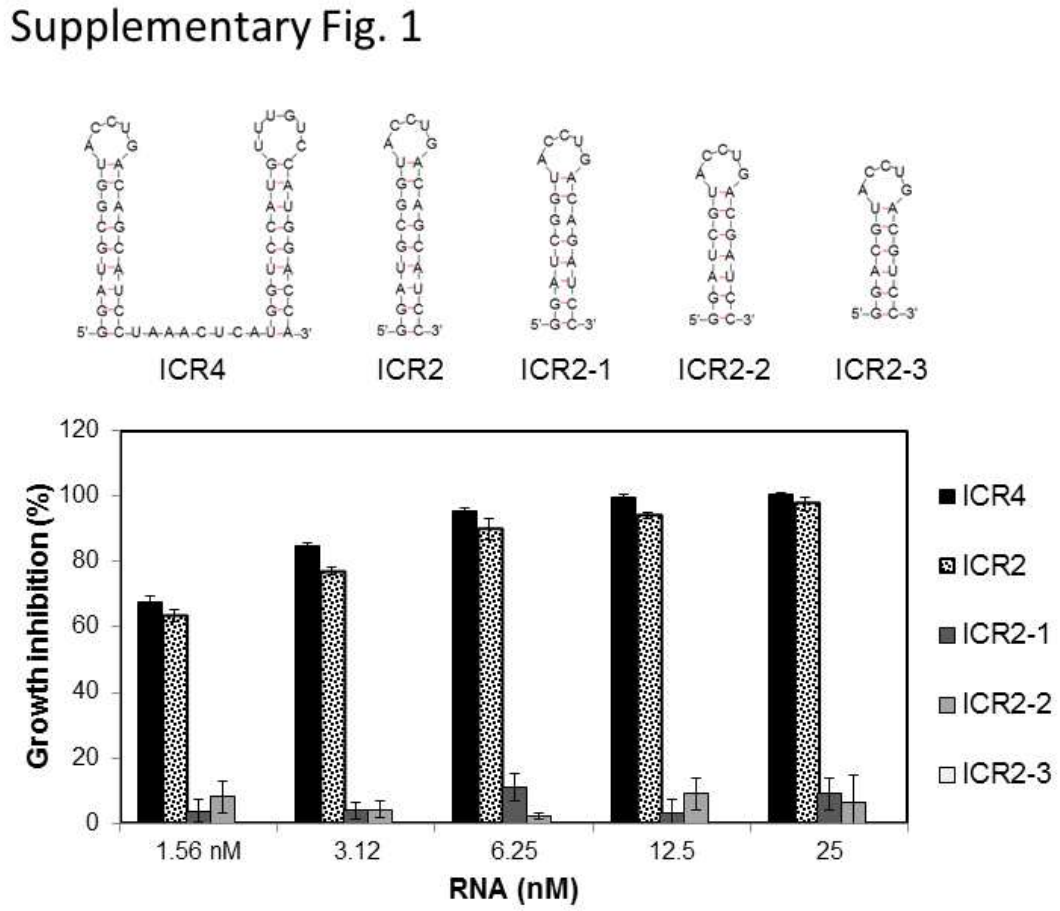

Supplementary Figure S1. Cytotoxicity of 5'ppp 2'F hairpin RNAs with 6-9 bp. WM266-4 cells were transfected for 4 h with ICR4, ICR2 and ICR2 with various truncations at indicated concentrations. Cell growth rate were determined at 3 days after transfection by MTS assay. Error bars are S.D..

Supplementary Fig. S2

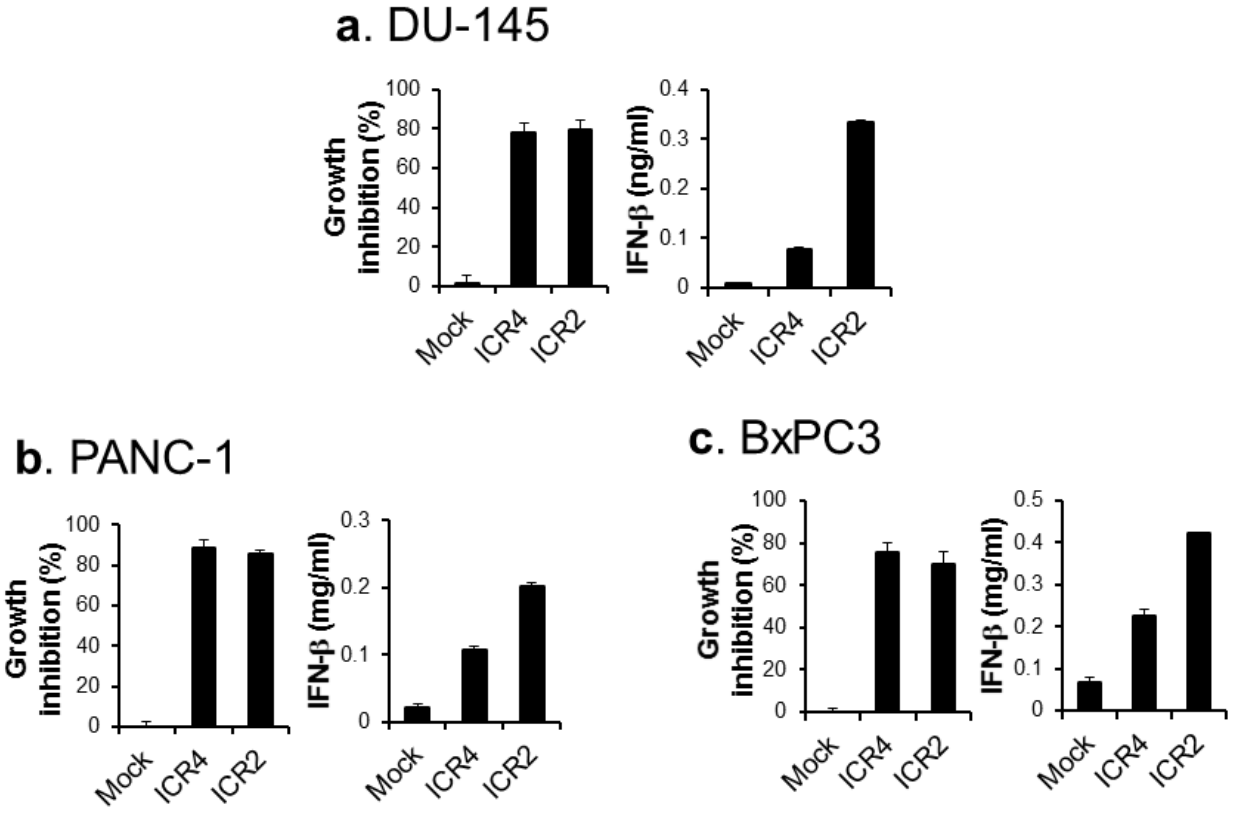

Supplementary Figure S2. Differential induction of IFN-β expression and growth inhibition of human prostate and human pancreatic cancer cells by ICR2 and ICR4. DU-145 human prostate cancer cell line (**a**), PANC-1 human pancreatic cancer cell line (**b**) and BxPC3 human pancreatic cancer cell line (**c**) were transfected with ICR2, ICR4 (1 μg/ml each) or transfection reagent alone (Mock). Cell growth and IFN-β production were determined by MTS assay and ELISA, respectively. Error bars are S.D..

Supplementary Fig. S3

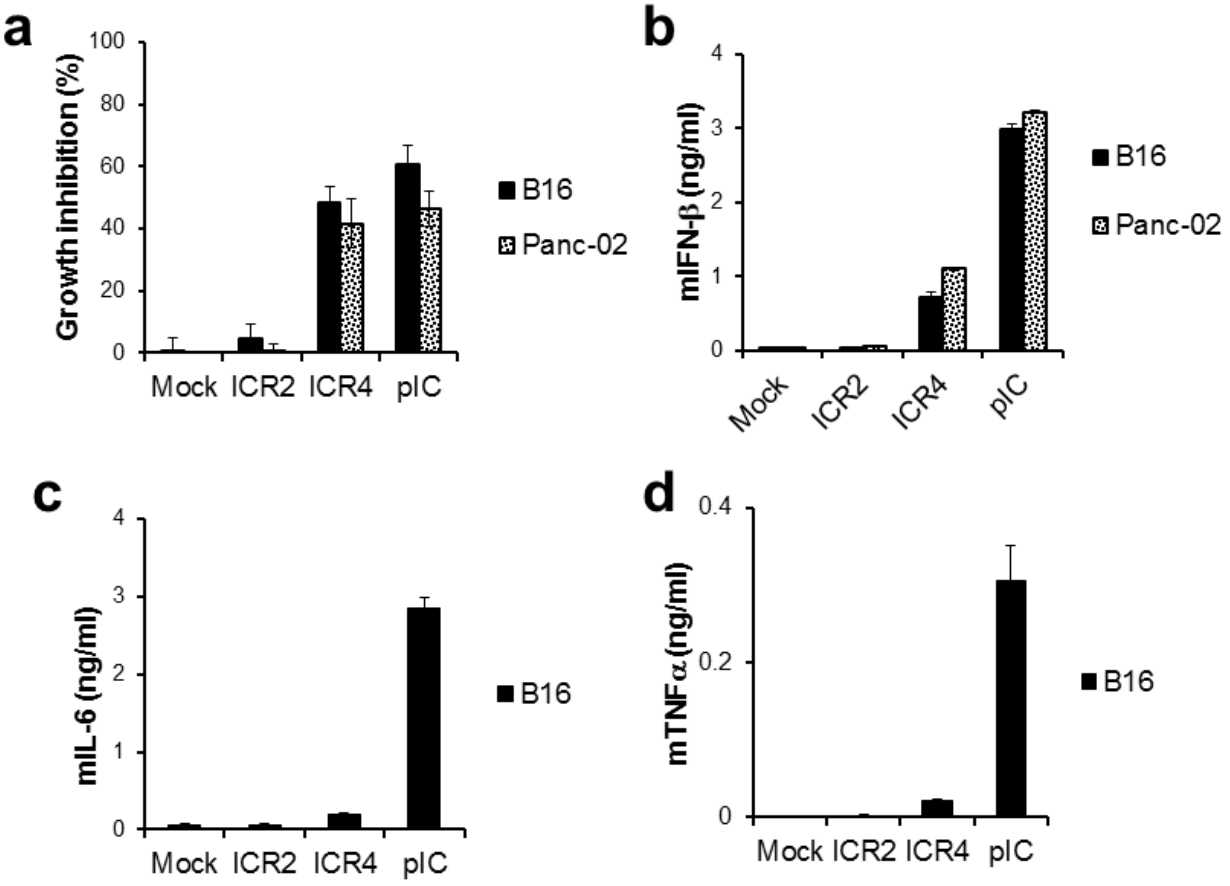

Supplementary Figure S3. Cytotoxicity and cytokine production by mouse cancer cells transfected with ICR2, ICR4 and polyI:C. B16 mouse melanoma cell line and PANC-02 mouse pancreatic cancer cell line were transfected with transfection reagent alone (Mock), ICR2, ICR4 or polyI:C (pIC) (1 μg/ml each). Cells and culture supernatants were harvested at 3 days after transfection. (**a**) Cell growth and production of (**b**) IFN-β , (**c**) IL-6 and (**d**) TNFα were determined by MTS assay and ELISA, respectively. Error bars are S.D..

Supplementary Fig. S4

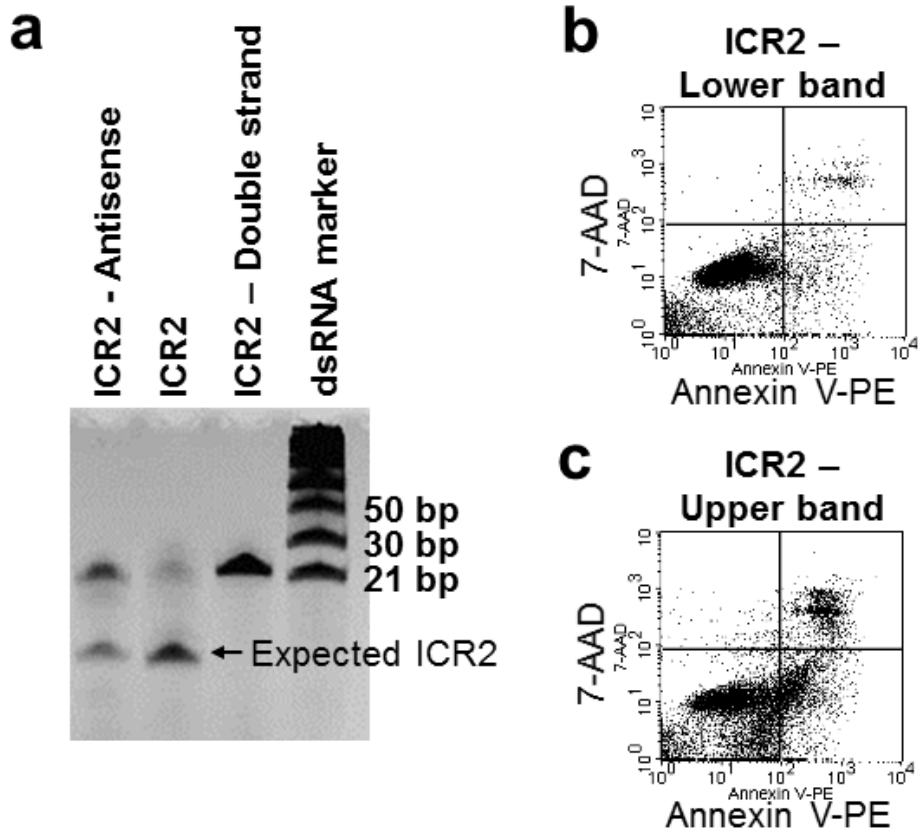

Supplementary Figure S4. Generation of T7 polymerase-induced IVT byproduct. (**a**) ICR2 and ICR2 antisense complementary to ICR2 were generated by T7 polymerase-induced IVT. ICR2-double strand was generated by hybridization of ICR2 and ICR2 antisense. RNAs were analyzed on 20% polyacrylamide gels. (**b**) Lower and (**c**) upper bands of ICR2 IVT were purified and transfected into human melanoma cell line WM266-4. Cell death levels were determined one day after transfection by Flow Cytometry-Based Annexin V-PE/7-AAD Staining Analysis.

Supplementary Fig. S5

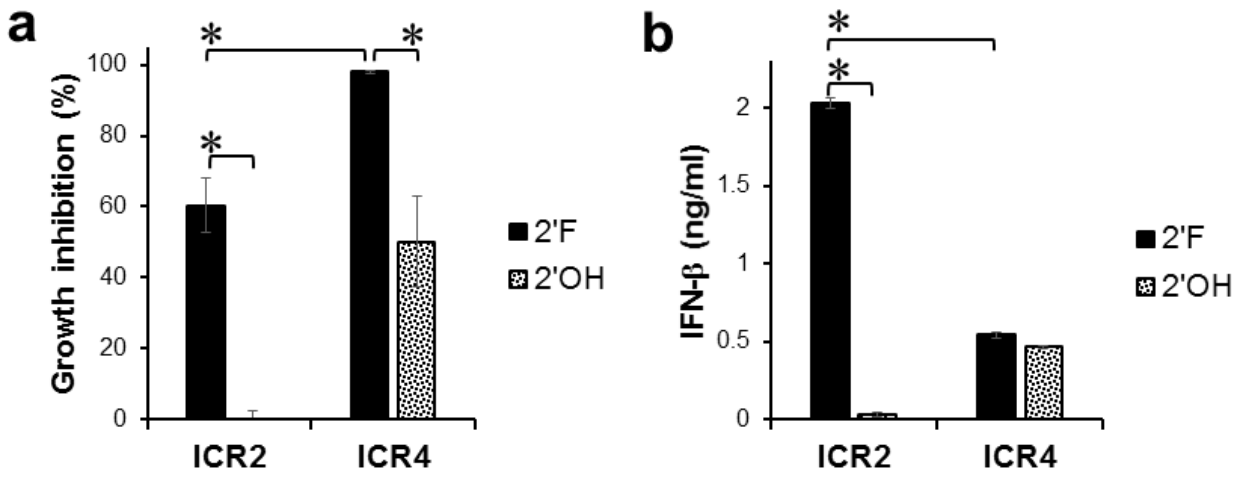

Supplementary Figure S5. Comparison of cell death- and IFN-β-inducing activities of ICR2 and ICR4 containing 2'F pyrimidine but 2'OH pyrimidine. WM266-4 cells were transfected with 2'F ICR2, 2'OH ICR2, 2'F ICR4 or 2'OH ICR4 (35 nM each). (**a**) Cytotoxicity and (**b**) IFN-β production was assessed at 72 h post transfection. Error bars represent the S.D. ∗ $P < 0.05$.

Supplementary Fig. S6

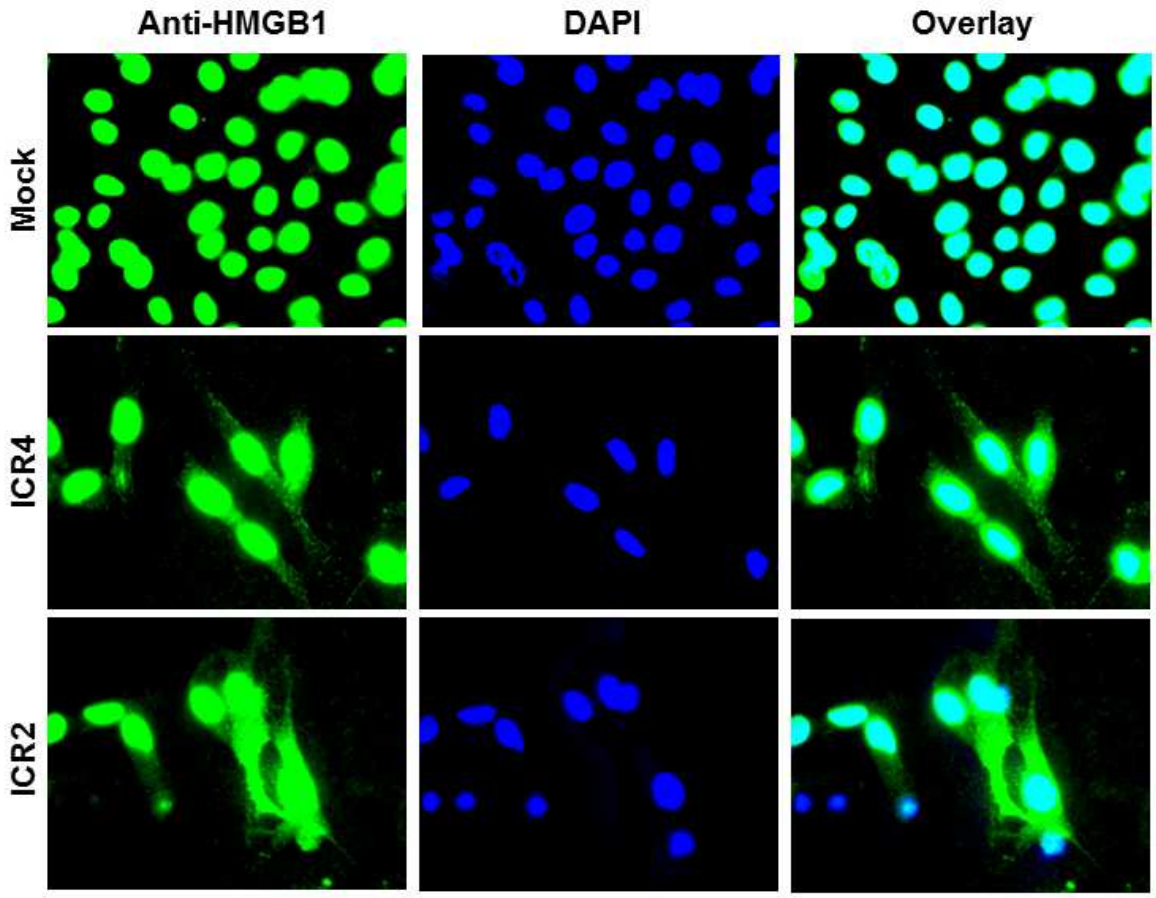

Supplementary Figure S6. Cytoplasmic translocation of nuclear protein HMGB1 in cells transfected with ICR2 and ICR4. WM266-4 cells were transfected for 4 h with ICR2, ICR4 or transfection reagent alone (Mock). Cells were harvested at 24h after transfection and co-stained with anti-HMGB1 (Green) and DAPI (blue). The expression of nuclear and cytoplasmic HMGB1 and nuclear DAPI was detected by fluoresce microscopy.

Supplementary Fig. S7

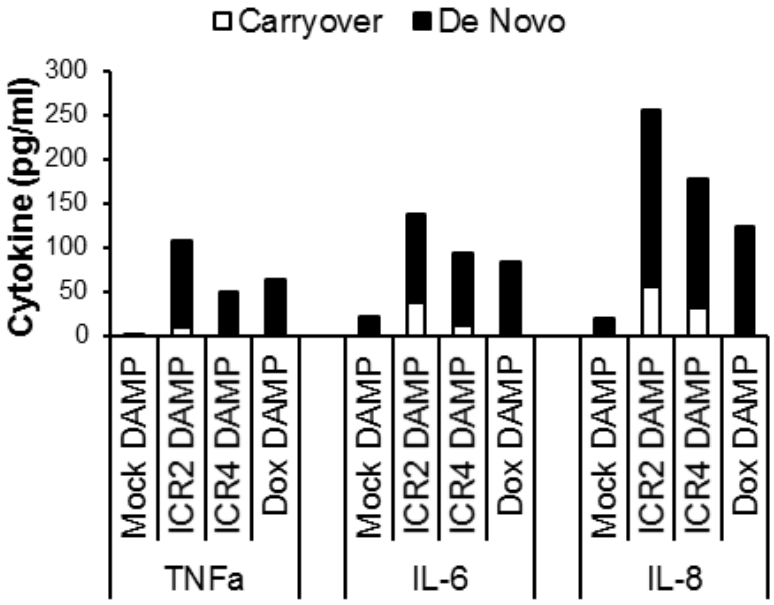

Supplementary Figure S7. Human DCs stimulated with DAMPs produced cytokines. Human PBMC-derived immature DCs were stimulated with DAMPs isolated from WM266-4 cells treated with transfection reagent alone (Mock DAMP), ICR2 (ICR2 DAMP), ICR4 (ICR4 DAMP) or doxorubicin (Dox DAMP). De novo production of TNFα, IL-6 and IL-8 by stimulated DCs (De Novo) and pre-existing cytokines in DAMPs (Carryover) were determined by ELISA.

Supplementary Fig. S8

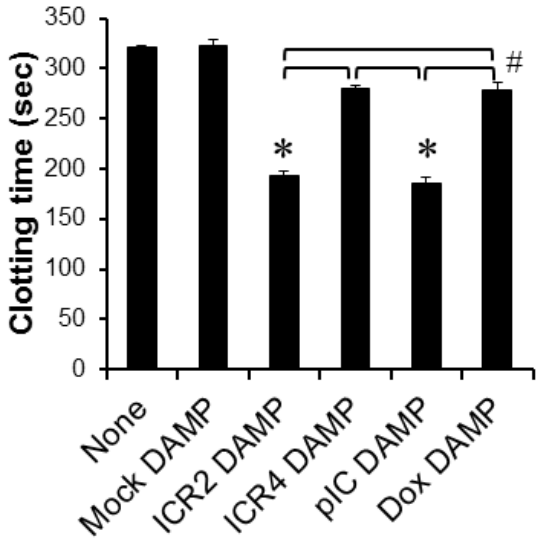

Supplementary Figure S8. Release of pro-coagulative DAMPs from human cancer cells treated with immunogenic cell death inducing agents. Enhancement of human plasma coagulation by DAMPs released from cells treated with transfection reagent alone (Mock DAMP), ICR2 (ICR2 DAMP), ICR4 (ICR4 DAMP), polyI:C (pIC DAMP) and Doxorubicin (Dox DAMP) was determined by coagulation assay. n=3, Error bar are S.D.. # $P < 0.05$ (indicated comparison). ∗ $P < 0.05$ (*vs* normal plasma clotting time (None)).

Supplemental Table

Table S1. RNA sequences.

RNA	Sequence (5'→3')
ICR1	ggaugcgguaccugacagcauccua
ICR1A	ggaugcgguaccugacagcauccuaaagug
ICR1B	ggaugcgguaccugacagcauccuaaaguggguggaagugag
ICR1C	ggaugcgguaccugacagcauccuaaaguggguggaagugagugagugaaauaaaaa
ICR2-	ggacguaccugacgucc
ICR2-	ggaucguaccugacgaucc
ICR2-	ggaucgguaccugacagaucc
ICR2	ggaugcgguaccugacagcaucc
ICR2A	ggacgaugcgguaccugacagcaucgucc
ICR2B	ggaugcgguaccugacagcauccaccugggaugcugucagguaccgcaucc
ICR3	ggagcggaugcgguaccugacagcaucc
ICR3A	ggggaggacagcggaugcgguaccugacagcaucc
ICR3B	ggaaugaggggaggacagcggaugcgguaccugacagcaucc
ICR3C	ggguaagugaaugaggggaggacagcggaugcgguaccugacagcaucc
ICR4	ggaugcgguaccugacagcauccuaaacucaugguccauguuuguccauggacca
ICR4A	ggaugcgguaccugacagcauccuaaacucaugguccauguuuguccauggaccaacuaccgacauuguauguguugauauaaaugu
ICR5	ggaugcgguaccugacagcauccugaguuuaguuguugu + ggaugcgguaccugacagcauccacaacaacuaaaacuca
ICR-L	gguuuuuuuuuuuuuuuuuuuu

Supplemental Materials and Methods

Enzyme-linked immunosorbent assay (ELISA)

TNF-α, IL-6 and IL-8 were determined using BD OptEIA™ ELISA sets (BD Biosciences, Franklin Lakes, NJ). IFN-β production was determined using IFN-β ELISA kit (PBL Biomedical Laboratories, Piscataway, NJ). HMGB-1 secretion was determined using HMGB1 ELISA kit (Tecan, Morrisville, NC) by following the manufacturer's instructions.

Immunoblot analysis and antibodies

Mitochondria and nuclear fractions were isolated using Mitochondria Isolation kit and NE-PER Nuclear Extraction reagent, respectively, (both from Thermo Scientific). Mitochondrial lysates, nuclear lysates and total cell lysates were prepared in 1x RIPA buffer (Sigma, St. Louis, MO) in the presence of the complete protease inhibitor cocktail and phosphatase inhibitor cocktail (Sigma). 30 µg of protein lysates were electrophoretically separated on 4-20% Mini-PROTEAN® TGX™ polyacrylamide gels (Bio-Rad, Hercules, CA) and transferred to polyvinylidene fluoride (PVDF) membranes (PolyScreen®, PerkinElmer). After rinsing in TBST20, membranes were blocked for 1 h in 5% dry milk in TBTS20, followed by overnight incubation with primary antibodies anti-XIAP (1:1000) (3B6; Cell Signaling, Danvers, MA), anti-TRAIL (1:1000) (C92B9; Cell Signaling), anti-phospo (p)-IRF-3 (1:500) (4D4G; Cell Signaling), anti-cleaved caspase-3 (1:200) (D3E9; Cell Signaling), anti-caspase-7 (1:200) (Cell Signaling), anti-NF-κB p65 (1:1,000) (L8F6; Cell Signaling), anti-RIP (1:1,000) (Cell Signaling), anti-RIG-I (1:500) (D14G6; Cell Signaling, Danvers, MA), anti-MDA5 (1:500) (D74E4; Cell Signaling) and anti-PKR (1:350) (Catalog No 3072; Cell Signaling). When

different proteins were sequentially detected on the same membrane, membranes were treated for 8 minutes with Restore Western Blot Stripping Buffer (Thermo Scientific, Rockford, IL), washed, blocked and probed again, as described above. Primary antibodies were detected using horseradish peroxidase (HRP)-conjugated anti-rabbit (1:2,000) (Cell Signaling) or anti-mouse (1:2,000) (Cell Signaling) secondary antibodies. Anti-β-Tubulin (1:1,000) (9F3; Cell Signaling), anti-CoxIV (1:1,000) (3E11; Cell Signaling) and anti-Histone H3 (1:1,000) (D1H2; Cell Signaling) were used as loading controls. HRP activity was visualized using the Western Lightning Plus Kit (PerkinElmer, Waltham, MA).

Detection of surface Calreticulin and cytoplasmic HMGB-1

The expression of surface Calreticulin was determined by flow cytometry after co-staining with anti-Calreticulin-PE (1/100 dilution) (Abcam, Cambridge, MA) and 7-AAD (BD Biosciences). For the detection of HMGB1, cells were fixed with a 4% paraformaldehyde solution followed by blocking and permeabilization with 5% BSA, 0.2% Triton X-100 in PBS, and stained overnight with anti-HMGB1 (1/1000 dilution) (Abcam), Alexa Fluor 488-conjugated goat anti-rabbit IgG (1/1000 dilution) (Abcam) was used as a secondary antibody. DAPI (4',6-Diamidino-2-phenylindole) (Sigma) was used as a nuclear counterstain. The expression of HMGB1 and DAPI was observed under a Zeiss Axio Observer microscope, and the images were analyzed using MetaMorph software (Sunnyvale, CA).

Clotting assay

5 µl DAMPs or culture media were mixed with 50 µL normal pooled human plasma (George King Bio-Medical Inc., Overland Park, KS). The mixture was incubated for 3 min at 37 °C, followed by the addition of 50 µL $CaCl_2$ (25 mM). Clotting times were recorded using STart®

Hemostasis Analyzer (Diagnostica Stago, Parsippany, NJ).